Co-occurring wintertime flooding and extreme wind over Europe, from daily to seasonal timescales

Article

Published Version

Creative Commons: Attribution 4.0 (CC-BY)

Open access

It is advisable to refer to the publisher's version if you intend to cite from the work. See Guidance on citing.

To link to this article DOI: http://dx.doi.org/10.1016/j.wace.2023.100550

Publisher: Elsevier

Co-occurring wintertime flooding and extreme wind over Europe, from daily to seasonal timescales

Bloomfield H.C. [a,*], Hillier J. [b], Griffin A. [c], Kay A.L. [c], Shaffrey L.C. [d,e], Pianosi F. [f,g], James R. [a], Kumar D. [d,e], Champion A. [h], Bates P.D. [a,g]

[a] *School of Geographical Sciences, University of Bristol, University Road, Bristol, BS8 1SS, UK*
[b] *Geography, Loughborough University, Loughborough, LE11 3TT, UK*
[c] *UK Centre for Ecology and Hydrology, Wallingford, OX10 8BB, UK*
[d] *Department of Meteorology, University of Reading, Whiteknights Road, Reading, RG6 7BE, UK*
[e] *National Centre for Atmospheric Science, University of Reading, Whiteknights Road, Reading, RG6 7BE, UK*
[f] *Department of Civil Engineering, University of Bristol, University Road, Bristol, BS8 1SS, UK*
[g] *Cabot Institute, University of Bristol, University Road, Bristol, BS8 1SS, UK*
[h] *AON, The Aon Centre, 122 Leadenhall Street, London, EC3V 4AN, UK*

ARTICLE INFO

ABSTRACT

The risk posed by heavy rain and strong wind is now suspected to be exacerbated by the way they co-occur, yet this remains insufficiently understood to effectively plan and mitigate. This study systematically investigates the correlations between wintertime (Oct–Mar) extremes relating to wind and flooding at all timescales from daily to seasonal. Meteorological reanalysis and river flow datasets are used to explore the historical period, and climate projections at 12 km resolution are analysed to understand the possible effects of future climate change (2061–2080, RCP 8.5). A new flood severity index (FSI) is also developed to complement the existing storm severity index (SSI). Initially, Great Britain (GB) is taken as a comparatively simple yet informative study area, then analysis is extended to the full European domain.

Aggregated across GB, wind gusts and precipitation correlate strongly (r_s ~0.6–0.8) at timescales from daily to seasonal, but peak around 10 days. A later peak is seen when considering correlations between wind gusts and river flows (40–60 days). This time is likely needed for catchments' soils to saturate. A conceptual multi-temporal, multi-process model of GB wintertime flood-wind co-occurrence is proposed as a basis for future investigation. When historical analysis is extended across Europe we find the timescale of maximum correlation varies strongly between nations, likely as a result of different meteorological drivers.

Impact focused correlation (FSI–SSI) is lower (r_s ~0.2) but increases notably with climate change at timescales of ~40 days (r_s ~0.4). Tentatively, very severe episodes (i.e., both >99th percentile) appear heavily influenced by climate change, increasing roughly threefold by 2061–2080 (p < 0.05). The return period of such an event is 16 years historically (compared to 56 years if the two hazards were independent), reduces to 5 years in future. Such metrics provide actionable information for insurers and other stakeholders.

1. Introduction

During winter, inland flooding and extreme wind are two of the hazards to most severely impact north-west Europe (Mitchell-Wallace et al., 2017). Although to climate scientists it might seem self-evident that these hazards are related, they are typically modelled independently in risk analyses. Evidence that they tend to systematically co-occur (Hillier et al., 2015; Martius et al., 2016; Owen et al., 2021b) is becoming increasingly robust (see Fig. 1 for examples) with the possibility that this significantly exacerbates joint risk. However, neither the interplay of hydro-meteorological mechanisms that give rise

to the co-occurrence, nor key timescales impacted, are yet fully understood. Most evidently, infrastructure operators, government agencies and (re)insurers are interested in distinct events (e.g., storms, with a maximum duration or *hours clause* of 5 days) or planning horizons (e.g., financial or regulatory years), although stresses on resources such as maintenance crews during intermediate periods can readily be imagined during weeks of adverse weather (White et al., 2022). Thus, co-occurrence within a range of time-windows is important.

Case studies of strong storms have securely established that both wind and flood damage might co-occur during the same weather system. Examples include storm Kyrill in 2007 (Fink et al., 2009), the

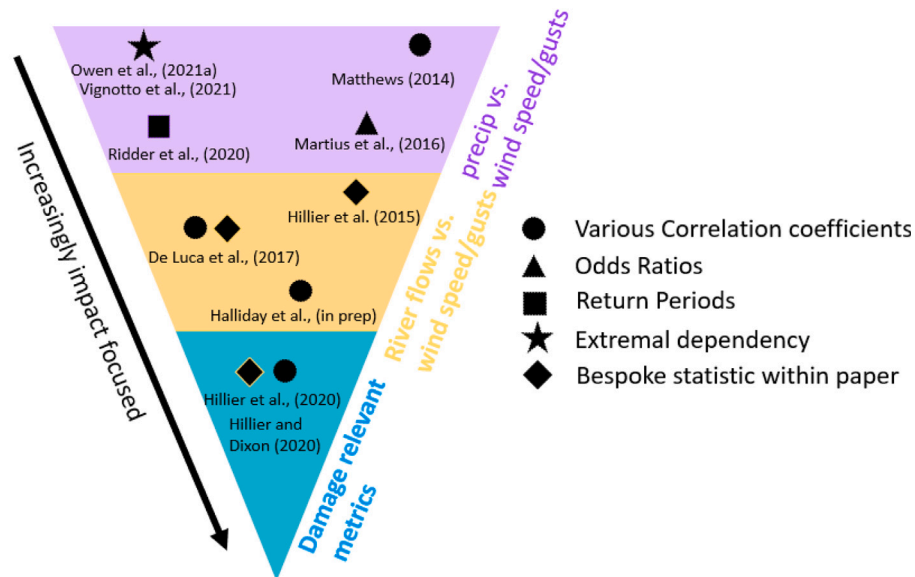## GB COMPOUND FLOOD-WIND LITERATURE METHODS SUMMARY

Fig. 1. A pictorial overview of methods applied to quantify compound wind extreme and flooding events across Europe within increasingly impact-focused datasets. We note most papers include multiple metrics, the most relevant results to our current work have been chosen.

19th January 2013 windstorm (Liberato, 2014) and storm Desmond in 2015 (Otto et al., 2018). A systematic relationship between flooding and extreme wind in NW Europe was first demonstrated by three papers (Matthews et al., 2014; Hillier et al., 2015; Martius et al., 2016), which also clearly illustrate the spectrum of contrasting, complementary approaches in use then and subsequently.

To identify the winter of 2013–2014 (Dec–Feb) as notably wet and stormy (Matthews et al., 2014) tracked extra-tropical cyclones (ETCs) in reanalysis products from 1871–2012 within the Iceland–UK domain. A seasonal 'storminess' metric (I) was developed and correlated with mean England–Wales precipitation using Pearson's r (r_p). Visually, r_p is 0.7 ± 0.1 (p < 0.05). As part of defining Great Britain's (GB's) exposure to multi-hazard risks, Hillier et al. (2015) moved from meteorological measures (e.g., precipitation) to ascertain that co-occurrence extends to annual (Nov–Oct) impacts. Conclusions were based on evidence from a blend of insurance losses (1998–2013; ABI, Association of Bristish Insurers, 2014) and hydro-meteorological observations (1958–2008). Flooding and wind extremes over a threshold are found to occur ~1.5 times more than expected, with joint 16-year return period losses higher by 20%–30% than if the hazards were independent.

In contrast, Martius et al. (2016) focus on near-surface wind and precipitation extremes, and short time-scales, mapping co-occurrence within a 72 h window for ERA-interim. Notably high percentages of co-occurring extremes are detected along the North-western coasts of Europe (e.g., Iberia, Norway), but are muted in other locations, and again ETCs are invoked as the explanatory process. Owen et al. (2021b) focus on short time windows to determine that co-occurrence in some places (e.g., GB, Norway) is typically within 1 h, and 70% of co-occurrences happen whilst an ETC is within 1110 km.

Recent work for GB from De Luca et al. (2017) uses peak river flow data for 260 basins in Great Britain (1975–2014) to distinguish large multi-basin floods at a spatial scale that is comparable to ETCs (e.g., ~1000 km). Analyses at 1–19 days and seasonal timescales, combined with a variety of meteorological indices were used to start to understand where 'memory' (Hillier et al., 2015) and time-lags in the hydro-meteorological system might arise. Seasonally, these multi-basin flood events correlate with numerous very severe gales ($r_p = 0.41$, p < 0.05). In addition, Hillier et al. (2020) demonstrated an increase in joint seasonal impact on infrastructure (rail network) due to flood-wind dependence of 27.8%.

A key limitation to the previous studies is the limited ability to comment on truly rare events given the length of the reanalysis/observational record. To attempt to overcome this, the UNSEEN method (Thompson, 2017) has been used, involving multiple realisations of the last 20–30 years using seasonal hindcast models to create a synthetic 600 year record (Hillier and Dixon, 2020; Owen et al., 2021a). Seasonal impact-based measures for flood and wind have suggested that extremes can be captured well (e.g., Spearman's rank correlation (r_s) of up to 0.54 found in Hillier and Dixon, 2020). However, caution is needed over orography (Owen et al., 2021a; Ridder et al., 2021), and there is the possibility that higher-resolution simulations may even be better than reanalysis products such as ERA5 (Zscheischler et al., 2021).

In summary, there is an obvious limitation in the literature, which would benefit from a study that spans timescales from hourly (Owen et al., 2021b) to seasonal (Hillier and Dixon, 2020). A consistent application of techniques to a variety of data types (e.g., flow gauge, reanalysis, climate model ensembles) representing quantities along the progression from meteorological quantities to hazard and risk is also needed. Specifically, as a step towards better understanding the co-occurrence of flooding and extreme wind across North-Western Europe, this paper applies consistent methods to a variety of datasets and timescales to investigate the following research questions:

1. What are the key timescales of correlation for extreme precipitation and wind, and why?
2. Are these also the key timescales of interest in more impact-based metrics?
3. How are these results impacted by climate change?

Great Britain (GB) is selected as an initial case study for these questions. It is a region exposed to winter storms destined for mainland Europe whilst being a relatively simple system, with rapid river response times (i.e., < 40 h; De Luca et al., 2017) and snow melt a limited influence. Following this, the results are extended to cover Europe.

2. Data and methods

In the following subsections the observed meteorological data (Section 2.1) and climate model data (Section 2.2) used to create meteorologically derived proxies for wind and flood risk are discussed.

Table 1
Details of hydro-meteorological datasets used within this study.

Dataset	Fields used (units)	Spatial resolution	Time period	Reference
ERA5	hourly total precipitation (mm), hourly instantaneous 10 m wind gusts (ms^{-1})	~30 km	1979–2021	Hersbach et al. (2020)
GLOFAS	daily river discharge (m^3)	~10 km	1979–2021	Harrigan et al. (2020)
CAMELS-GB	daily-mean river discharge (m^3)	671 GB stations	1970–2015	Coxon et al. (2020)
CHESS-MET	daily mean total precipitation (mm), daily mean 10 m wind speeds (ms^{-1})	1 km	1970–2015	Robinson et al. (2016)
UKCP Regional	daily max 10 m wind gust (ms^{-1}) Model daily total precipitation (mm)	12 km	1981–2000 2061–2080	Tucker et al. (2022)
UKCP Grid-to-Grid	river flows (m^{3}s^{-1})	1 km	1981–2020 2061–2080	Kay (2021) Griffin et al. (2022a)

Following this National Rail impact data is described, which forms a damage relevant comparison to our derived estimates (Section 2.3). Table 1 summarises all the meteorological datasets used. Following this, assessment of the co-occurrence of wind and precipitation extremes is reviewed in terms of relevant statistical measures (Section 2.4) and the plausible metrics which range from essentially climatic to those which relate more directly to risk or impact (Section 2.5).

All metrics used in this study are calculated during extended winter (October–March) and nationally aggregated. When using the UK Climate Projections Data (UKCP), thresholds defined for historical data (1981–2020) are applied to both present and future climate to understand potential changes.

2.1. Observed meteorological data

To assess the co-occurrence of extreme wind and precipitation events over GB, multi-decadal records of meteorological data are required. Reanalysis data products are a useful tool to provide this kind of information. The primary historical data used in this paper is the ERA5 reanalysis (Hersbach et al., 2020). ERA5 is based on the European Centre for Medium Range Weather forecasting's Integrated Forecasting System (IFS) cycle Cy41r2, which was operational in 2016.

To complement the ERA5 data, daily total river discharges are taken from the Global Flood Awareness System (GLOFAS) (Harrigan et al., 2020). This dataset is simulated by forcing the LISFLOOD hydrological modelling chain with inputs from the ERA5 reanalysis; see Hirpa et al. (2018) for further details of the model framework setup and calibration. It is therefore compatible with other outputs from ERA5 used here. GLOFAS is, however, considered relatively coarse when modelling river flows. The quality of a reanalysis product compared to observed data could also be questioned. To complement the analysis using ERA5 and GLOFAS, daily river flow, precipitation and 10 m wind speed data from 671 catchments across GB, created as part of the CAMELS-GB dataset is also used (Coxon et al., 2020). The wind speed and precipitation data used in CAMELS-GB is taken from CHESS-MET (Robinson et al., 2016) which is a 1 km gridded product available over the UK; see Table 1 and Appendix A for further details.

2.2. Climate model data

Using observed meteorological data only allows for a small selection of possible extreme wind and precipitation events to be analysed. Climate model simulations present an opportunity to consider plausible, but as yet unrealised, alternatives. However, climate models need to be fully evaluated to ensure that they represent the essential processes that give rise to extreme winds and precipitation events. In this study the UK Climate Projections 2018 (UKCP18, from hereon referred to as UKCP) regional model simulations are chosen for analysis. The UKCP simulations have been used for a number of impact studies and have been shown to have a good representation of historical precipitation (Lowe et al., 2018; Cotterill et al., 2021; Tucker et al., 2022; Lane and Kay, 2021) and wind gusts (Manning et al., 2021) when compared to lower resolution climate model simulations and gridded observations.

The regional simulations provide hourly data over the same area as the commonly used EURO-CORDEX domain Jacob et al. (2014). Simulations run from 1980–2080 using the Representative Concentration Pathway (RCP) 8.5 climate change scenario, and the setup of the 12 member perturbed parameter ensemble is described in detail in Tucker et al. (2022). Hourly instantaneous wind gusts and total precipitation are taken from all 12 ensemble members for two periods, 1981–2000 and 2061–2080. Matching river flows are derived by using the UKCP precipitation and temperature data (and derived potential evapotranspiration data) to drive the Grid-to-Grid (G2G) hydrological model (Kay, 2021). The resulting daily mean river flows have been output on a 1 km grid over GB, and have been summarised nationally on a daily time step, to construct impact-based metrics (as outlined in Hillier and Dixon, 2020). Further details of the UKCP-based river flows are given in Griffin et al. (2022b).

2.3. National rail impact data

In the context of natural hazards, meteorological data are proxies, studied as they are argued to relate to extremes that have the potential to cause impacts. As a reality check, it is also therefore useful to consider observed impacts.

Network Rail (NR), who are the owner and infrastructure provider of most of the rail network in GB, record delays to trains. NR's hazard-coded Weather Related Incident Impact Data (WRIID) contains ~274,000 incidents (2006–2019) that have each been assigned to a hazard and impact location (the originating site of delays). It is at a resolution of typically ~10 min and <5 km. 72.5% of these costs occur in the winter half-year (Oct-Mar). Impact in WRIID is quantified financially (pounds sterling), derived from delay minutes, and additionally each incident is described qualitatively e.g., *fallen tree on line*. We make use of the number of incidents occurring due to extreme winds or flooding, and the costs associated with extreme winds or flooding in Section 3.1.

Whilst losses in the summer remain substantial, at this time flood-wind correlation in the WRIID data is negligible. This demonstrates that the categorisation used is robust. This is because if flood and wind were being confused or mixed a false correlation would be present, and it is difficult to imagine why this artefact would vary by season. Thus, the WRIID data overcame a limitation common in insurance data (see Hillier et al., 2015 Appendix B). The WRIID data have been used previously for work on heat Ferranti et al. (2016) and Ferranti et al. (2018) and seasonal multi-hazard analysis (Hillier et al., 2020), but not yet for the sub-seasonal examination of flooding and extreme wind. Data is aggregated (summed) to GB level for analysis here. Appendix B gives future information on the categorisation of flood-wind damage in WRIID.

2.4. Defining co-occurring events

The studies described in Section 1 use a range of methods to define the presence compounding perils, shown schematically in Fig. 1. The choice of approach is dependent on the nature of the research question. The three most common methods are:

- Pearson's correlation coefficient, r_p (e.g., Matthews et al., 2014; De Luca et al., 2017; Hillier and Dixon, 2020).
- The logistic regression model (e.g., Martius et al., 2016), which quantifies the odds-ratio (multiplicative factor) of predicting a precipitation extreme at a specific grid point given a wind extreme occurring.
- Extremal dependency measures based on co-occurrence or otherwise of wind and precipitation extremes above a given percentile. This was proposed by Coles et al. (1999), illustratively used in Hillier et al. (2015), Martius et al. (2016) and Owen et al. (2021b), and includes the idea of an occurrence ratio (i.e., observed number of co-occurrences divided by the number expected due to chance).

This list is not exhaustive, with other methods used including the examination of residual tail dependence (Vignotto et al., 2021) and more impact-based assessments such as a change in *Annual Exceedance probabilities* (the probability of annual aggregate losses exceeding a threshold; Hillier et al., 2015; Hillier and Dixon, 2020; Bevacqua et al., 2021).

A key aim of this study is to assess the relationship between extremes relating to flooding and wind damage across multiple timescales, to unify results from previous studies. To achieve this, the Spearman's rank (r_s) correlation is calculated within non-overlapping windows of varied length throughout the chosen datasets. Window length ranges from one day, as in Martius et al. (2016) and Owen et al. (2021b), out to 180 days as in Hillier and Dixon (2020). Spearman's rank is the main statistic deployed as it is a non-parametric metric that is simple, familiar and thus amenable to easy communication to varied stakeholders, and there is no indication that correlation disappears when moving from the body of the distribution into the tail (see Appendix C).

2.5. Impact-based metric definitions

To understand the complex relationship between wind and flood damage, a set of GB-aggregates have been developed ranging in a progression from weather to impact. The first metrics used are GB-aggregate total daily precipitation (P), maximum daily 10 m wind gusts (v) and total daily river flow (q). The daily data are then aggregated to the timescales used in the correlation analysis. P and q are aggregated through summation, whereas for v the mean of daily maxima is calculated over the period of interest. Population weightings for 2020 (Doxsey-Whitfield et al., 2015), when used, are applied to each grid cell of the meteorological data before aggregation. Population weightings here are used as a proxy for the location of assets at risk that would experience loss or damage from extreme weather.

The metrics used to most directly estimate impact in this study are the Storm Severity Index (SSI) and a new Flood Severity Index (FSI). The SSI was originally developed by Klawa and Ulbrich (2003a) and follows the form used in Pinto et al. (2012) and Priestley et al. (2018):

$$SSI(t) = \sum_{i=1}^{N_i} \sum_{j=1}^{N_j} (\frac{v(t)_{i,j}}{v_{i,j}^{98}} - 1)^3 \cdot I_{i,j} \cdot L_{i,j} \cdot pop_{i,j}$$

$$I_{i,j} = \begin{cases} 0 & \text{if } v(t)_{i,j} < v_{i,j}^{98} \\ 1 & \text{otherwise} \end{cases}$$

$$L_{i,j} = \begin{cases} 0 & \text{over sea} \\ 1 & \text{over land} \end{cases}$$

Here $v_{i,j}$ is the daily maximum wind gust at longitude i and latitude j. $pop_{i,j}$ is the 2020 population density in a given location, taken from Doxsey-Whitfield et al. (2015). N_i and N_j show the total number of longitudes and latitudes calculations are performed over respectively. Throughout the paper the SSI and FSI metrics are calculated at daily resolution (t = 1 day) and subsequently aggregated to longer temporal periods for correlation analysis. Therefore, $v_{i,j}^{98}$ always represents the gridded daily 98th percentile from October–March.

v^3 is a well-established proxy for damage (see Hillier and Dixon, 2020 for discussion), and v_{ij}^{98} is the local (i.e., per grid cell) 98th percentile, used as wind damage typically occurs over this threshold (Klawa and Ulbrich, 2003a; Priestley et al., 2018). Use of a daily 98th percentile allows for a comparison between datasets without the need for bias correction, which would be required were a fixed threshold used. It also facilitates an easy comparison with the CHESS-MET historical dataset (see Table 1) where only daily-mean 10 m wind speeds are available. The percentile threshold also accounts for local spatial variations in building construction on the assumption that buildings are generally constructed to be resistant to locally expected gust maxima.

The Flood Severity Index (FSI) is defined as:

$$FSI(t) = \sum_{i=1}^{N_i} \sum_{j=1}^{N_j} (\frac{q(t)_{i,j}}{q_{i,j}^{99.5}} - 1) \cdot I_{i,j} \cdot L_{i,j} \cdot pop_{i,j}$$

$$I_{i,j} = \begin{cases} 0 & \text{if } q(t)_{i,j} < q_{i,j}^{99.5} \\ 1 & \text{otherwise} \end{cases}$$

$$L_{i,j} = \begin{cases} 0 & \text{over sea} \\ 1 & \text{over land} \end{cases}$$

The form is developed from the SSI with parameters defined in the same way, except here the key hydro-meteorological variable is q, the daily total river flow. We note that FSI is always calculated at a daily timescale, using the 99.5th percentile of daily total river flows. A modified threshold is used for the damage and the cubic behaviour is removed to account for the differences in wind vs. flood damage. Population weightings are included as previously described for SSI to account for the increased amount of damage reported in large population centres.

Defining percentile thresholds for flood damage is difficult, as they are more diverse than those seen for wind damage (e.g., incorporating effects such as surface runoff, snow melt and landslides Williams, 1978; Martius et al., 2016). A complex trade-off emerged when designing the FSI metric between accurately selecting percentile exceedances associated with flood damage, and having enough years of data for statistically robust results (see Section 4.1 for further details).

Fig. 2 shows the relationship between FSI and the WRIID loss data from National Rail. This gives confidence that this metric is able to capture losses on an annual timescale, in the case of the number of floods the correlation is very high (0.74) with reductions seen when considering the costs associated with flooding (0.49). Further analysis (not shown) showed the ability of FSI to capture notable events, such as the February 2020 flooding associated with wind storms Dennis and Ciara. We note that, unsurprisingly, the metric struggles to capture very localised flooding events, such as the 2004 Boscastle flood. Appendix D gives an overview of the number of times recorded floods from the Chronology of British Hydrological Events (Black and Law, 2004) were found in the FSI dataset, giving further confidence that the metric can capture the most extreme events in the observed record.

3. Results

3.1. GB historical correlation analysis: progression from hydro-meteorology to impacts

Fig. 3a shows the Spearman's rank correlation between GB-average hydro-meteorology and impact variables at various timescales throughout October to March, 1979–2021 using ERA5 weather variables and
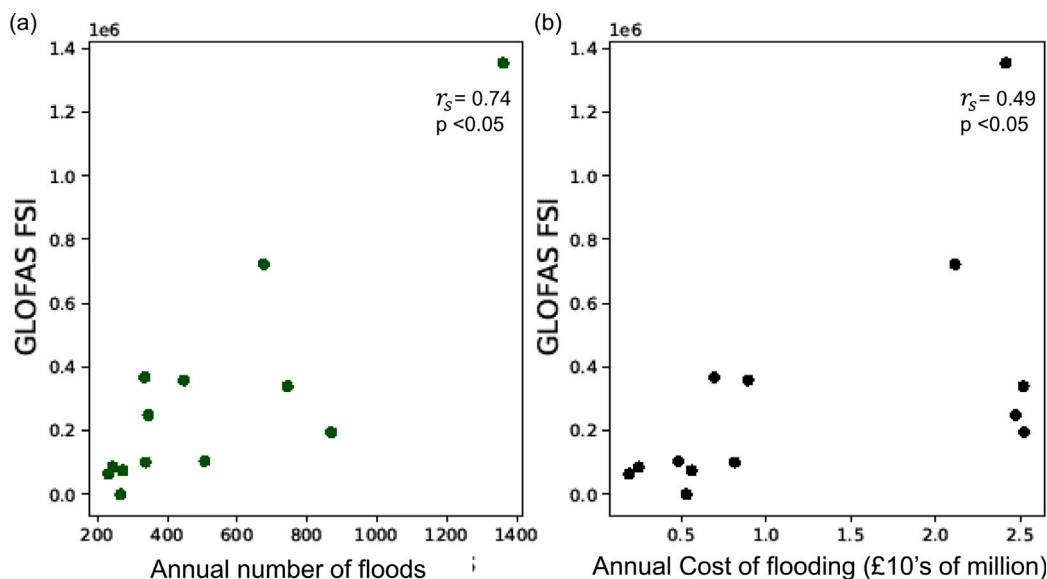
Fig. 2. Relationship between annual-aggregated wintertime FSI and GB National Rail flood data for years 2006–2018. (a) Number of floods. (b) Cost of flooding.

GLOFAS river flows. All grid boxes are equally weighted. (So the impact of population from the SSI and FSI equations is removed.) Equal weightings are examined first as population weightings may not be representative for all users (e.g., rail networks, telecommunications, power lines and crops). To calculate the Spearman's rank correlation over timescales greater than 1 day (the resolution of the underlying variables) the following rules are followed:

- The maximum daily 10 m wind gust is calculated over the required time period.
- Daily river flows and precipitation are summed over the required time period.
- The daily SSI and FSI are accumulated over the required time period.

Non-overlapping periods are used for analysis, so for example at the 180 day timescale, a maximum or sum for October–March data is calculated for each of the winters from 1980–2021, giving 41 data points.

The correlation between 10 m wind gusts and total precipitation is around 0.7 at all timescales, broadly agreeing with past studies that looked at various temporal scales from daily to seasonal (Matthews et al., 2014; Hillier and Dixon, 2020; Owen et al., 2021b). A peak correlation of ∼0.8 is seen with a 10 day window. Timescales on Fig. 3 are of key interest to the insurance sector. The first is 5 days. This is typically the period during which claims are attributed to a single windstorm including associated flooding. The second is 21 days. This is typically the period in which damage is accrued for an event classed as a flood.

For wind gusts and total river flow (gold line in Fig. 3a) correlation is lower (∼0.4) at daily timescales, similar to De Luca et al. (2017). After this it rises to a comparable level (∼0.65) at timescales of 40–60 days. This delay is likely associated with the wetting up of catchments over time (see Section 4.2). Therefore, while precipitation has been used as a proxy for flood damage in a number of previous short-term studies on compound wind-flood events (e.g., Martius et al., 2016; Owen et al., 2021b,a; Ridder et al., 2022; Li et al., 2022), these results highlight a potential to exaggerate the correlation between flooding and wind damage at lead times of less than ∼40 days.

The final set of lines on Fig. 3a show the correlation between SSI and FSI, which are indices more directly related to impactful extremes. Here correlation is ∼0.4, albeit with some indication of lower values at daily timescales and higher ones across seasons. This correlation is generally lower than reported in the literature, but differs from most studies in that it emphasises the correlation between the most extreme events across GB.

Including population weightings (Fig. 3b) causes a mild reduction (∼0.1) in correlation for all cases. Correlation between wind gusts and total precipitation drops to ∼0.6 at daily to weekly timescales, as more heavily populated regions have a weaker correlation than those over large orography (see Hillier and Dixon, 2020). Broadly, correlations in recorded losses due to wind and flood damage from National Rail (Fig. 3c) agree with those from GB-average total river flows vs mean maximum wind gusts, providing an additional justification for arguing that the proxies selected propagate into real-world impacts.

The choice of historical data product may influence the results. So, to robustly ascertain the correlations' presence, the analysis was repeated using observed river flow data from CAMELS-GB (1980–2015) and a 1 km reanalysis product CHESS-MET. A similar pattern of reducing correlations with increasingly impact-based metrics was found, Particularly when sub-setting to only use the 134 largest river catchments (i.e., the top 20%; see Appendix A).

3.2. GB historical extreme SSI and FSI

With only a 42 year observed period available, the ability to capture events extreme in both FSI and SSI is limited. It is possible however to investigate, separately for each metric, where and when events with the most extreme values of the metric occur. Fig. 4 shows for ERA5 and GLOFAS, the spatial distribution of occurrences of the top 1% and top 0.1% of SSI and FSI events. Here an event is limited to a daily value of each metric (note that no population weightings are applied here) although similar results are seen for 3-day accumulations.

Of the top 1% of SSI events (Fig. 4a) ∼70% of them affect grid cells across central and northern England, tapering to 30% over northern Scotland. The top 0.1% of SSI events support this idea (Fig. 4b). Nearly all (7 out of 8 events) occur over Northern England and Wales, implying a large footprint. Thus, the most extreme SSI events impact a large spatial region, most of GB. Fig. 4c shows that the most extreme SSI events are most likely in January and February, with the majority of the top 1% of events happening in December–February.

Conversely, only 30% of the top 1% of FSI events happen in the same location (Fig. 4d), implying they are much more localised. There is more spatial co-occurrence over the top 0.1% of FSI events, implying they are larger in area and are most common over the East coast
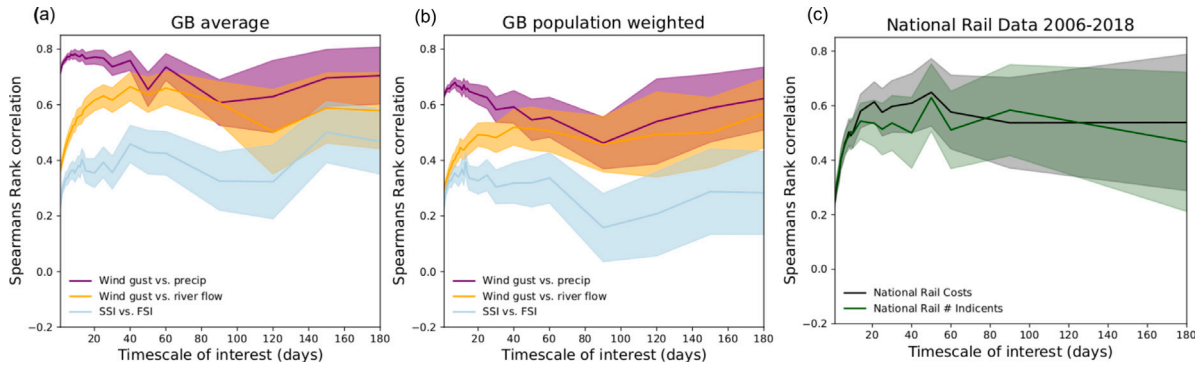
Fig. 3. Spearman's rank correlation between various metrics, at timescales from 1 to 180 days and aggregated across GB. ERA5 reanalysis and GLOFAS (a) with equal weighting given to all grid boxes and (b) with population weightings applied. (c) Correlation between number of events occurring due to extreme wind and flooding on the GB rail network (green) and correlation between costs due to extreme wind and flooding (grey). (For interpretation of the references to colour in this figure legend, the reader is referred to the web version of this article.)
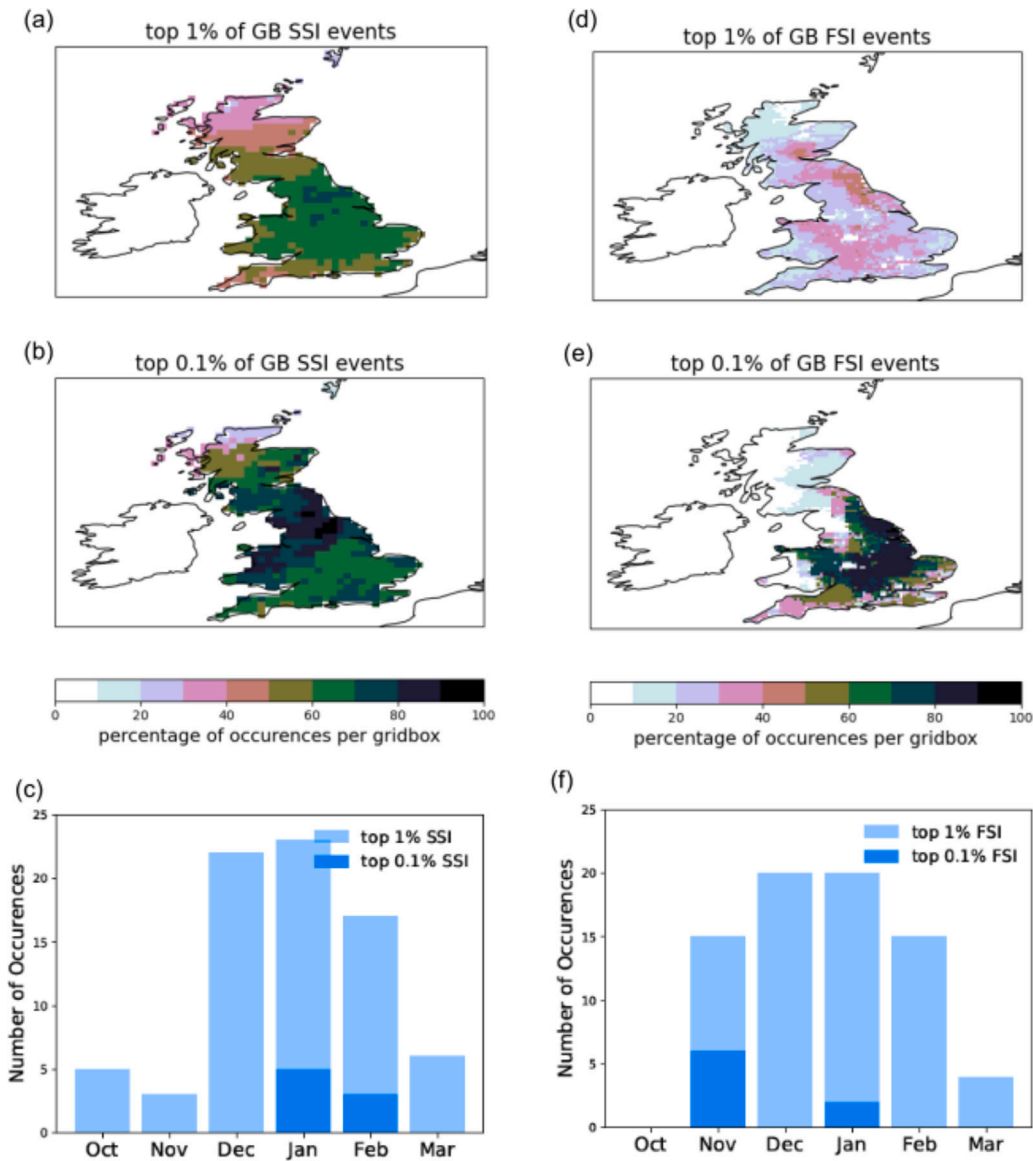

Fig. 4. Spatial occurrence of (a) the top 75 days (top 1%) of October–March SSI events from 1979–2021 in ERA5. (b) as (a) for the top 8 (top 0.1%) 1-day events. (c) Monthly occurrence of the most extreme SSI events. (d–f) as (a–c) for the FSI events from GLOFAS.

of England and central England (Fig. 4e). This supports observations from Quinn et al. (2019) which showed that the most extreme floods

in the USA often have a larger spatial footprint. The most extreme FSI events happened in November or January, with many more extreme
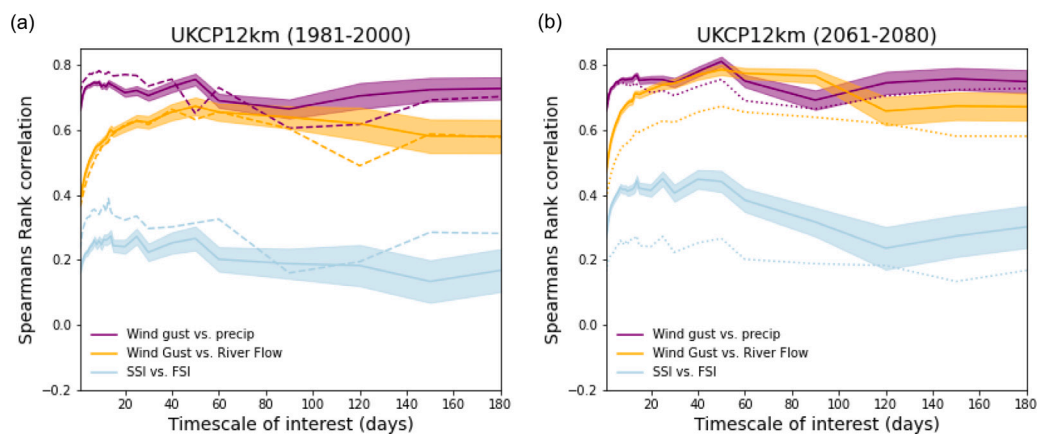
Fig. 5. GB-aggregate Spearman's rank correlation between various metrics (climate progressing to impact), at various timescales from 1 to 180 days from the UKCP regional simulations (a) for the present climate period 1981–2000 where dashed lines show ERA5 correlations from Fig. 3. We note SSI and FSI are population weighted. (b) for the future climate period 2061–2080. Dotted lines show the historical correlations from panel (a) for ease of comparison. Solid lines in both panels show the ensemble-mean correlation, shaded areas show two standard deviations of 2000 bootstrapped samples of the Spearman's rank correlation. Further details of datasets used are given in Table 1.

events in November than seen for SSI. Understanding the spatial variability of these extremes is important for understanding an insurer's portfolio of risk across multiple perils.

There are only two incidents when an extreme (top 1%) SSI event co-occurs with an extreme FSI event (i.e., a 1 in 20 year return period). These are the 7th February 1990 and 13th December 2000. The event on 7th February 1990 was associated with storm Judith, the second storm in a sequence of seven events, which ran from 25th January to 1st March 1990. Judith followed the notable storm Daria (Klawa and Ulbrich, 2003a). The 13th December 2000 was a time when 17 severe flood warnings were in operation across Southern England and a number of ferries were stranded in the English channel, again associated with stormy conditions (see *http://www.met.reading.ac.uk/brugge/diary2000.html*). It is interesting to note neither of these were wind storms associated with substantial losses, although this may be an artifact due to the temporal proximity to storm Daria (Klawa and Ulbrich, 2003a; Roberts et al., 2014). This analysis supports the idea that the largest wind events are not necessarily very wet (Hillier and Dixon, 2020) adding insight for flooding, and for the most extreme compound events across GB. This will be a topic of future investigation.

3.3. GB UKCP correlation analysis: historical and future

Fig. 5 shows an equivalent correlation analysis to Fig. 3a but for the UKCP 12 km ensemble. The historical correlations (Fig. 5a) between climate variables are similar to observations, albeit with reduced aleatory uncertainty (i.e., error bars) due to the larger sample size. The correlations between SSI and FSI are lower than those seen in the ERA5 data by ~0.1, particularly at short timescales. These results suggest that UKCP captures some of the processes responsible for the observed correlation between extreme flood and wind events.

When comparing the historical and future periods in UKCP there is a small but discernible increase in the correlation between total river flow and instantaneous wind gusts (Fig. 5b). Increased correlation is also seen between SSI and FSI at short timescales out to ~1 month. Unpacking this further shows that in the future period a moderate decrease in days with an SSI occurring (−2% p < 0.05), and a similarly sized increase in days with an FSI (+ 3% p < 0.05).

Table 2 presents results when focusing on the most extreme FSI and SSI days. The return period of exceeding the 95th percentile of SSI and FSI concurrently goes from 0.7 years at present, to 0.4 years in a future climate. In the historical period the co-occurrence of daily SSI and FSI jointly exceeding the 99th percentile has a return period of 13 years, which is reduced to only 4 years in the future period. This is evidence for an increasing probability of co-occurring extremes in the future, even if extreme SSI days may be a little less frequent.

3.4. Correlations across Europe

Although GB has been the focus of this paper notable differences are seen when the larger spatial domain of Europe is considered. Spearman's rank correlation between total river flows and 10 m wind gusts is selected to illustrate the results as it is most similar to the National Rail flood-wind correlations in Fig. 3c. Fig. 6 shows results for 37 European countries at daily, weekly, monthly and seasonal timescales. Different countries correlations peak at different timescales, presumably due to the contrasting driving processes. For example, on daily timescales, highest correlations are seen over GB and Ireland, likely due to their relatively isolated river networks. However, on seasonal timescales highest correlation is seen over Spain and Portugal with correlations exceeding 0.9.

Many previous studies used precipitation as a proxy for flooding, which we have shown is not always appropriate, at least for GB on timescales of <2 months. Specifically, Fig. 6 provides a means of advancing on previous interpretations as timescales are indicative of particular driving hydro-meteorological processes. Selected timescales and features of the maps are discussed in Section 4.4.

The key point to note is that the GB results, although useful, are not indicative of the full European response and a bespoke analysis is needed to capture the relationship between flood and wind damage in each country.

4. Discussion

Spearman's Rank correlation (r_s) has been used to robustly show the correlation between wintertime extremes associated with wind damage and flooding. In GB, r_s for historical times is 0.6–0.8, present within various proxies for hazard, reanalysis datasets, hydrological models, and impacts on rail infrastructure. To understand better how this may be used to estimate multi-sector impacts, a Flood Severity Index (FSI) to pair with the established storm Index (SSI) has been proposed and is further discussed in Section 4.1. The relative contributions of varied drivers of the co-occurrence of flooding and extreme winds can be assessed and assimilated into a conceptual model (Section 4.2). Furthermore, an extrapolation can be made into the future (Section 4.3) and the correlation analysis broadened across Europe (Section 4.4).

4.1. Flood Severity Index

When developing the FSI, a key decision point was the river flow exceedance threshold used to distinguish flooding. Critical thresholds for flooding depend on the duration of the event, the local precipitation

Table 2

Summary statistics for the co-occurrence of extreme SSI and FSI events that exceed the stated percentiles for historic (1981–2000) and future (2061–2080) climate in UKCP. The first two columns are the number and return period (RP) of events expected if the FSI and SSI were independent. The Ratio is the number of simulated events divided by the number expected if the two variables were independent. All results are significant (p < 0.01, using a binomial distribution.).

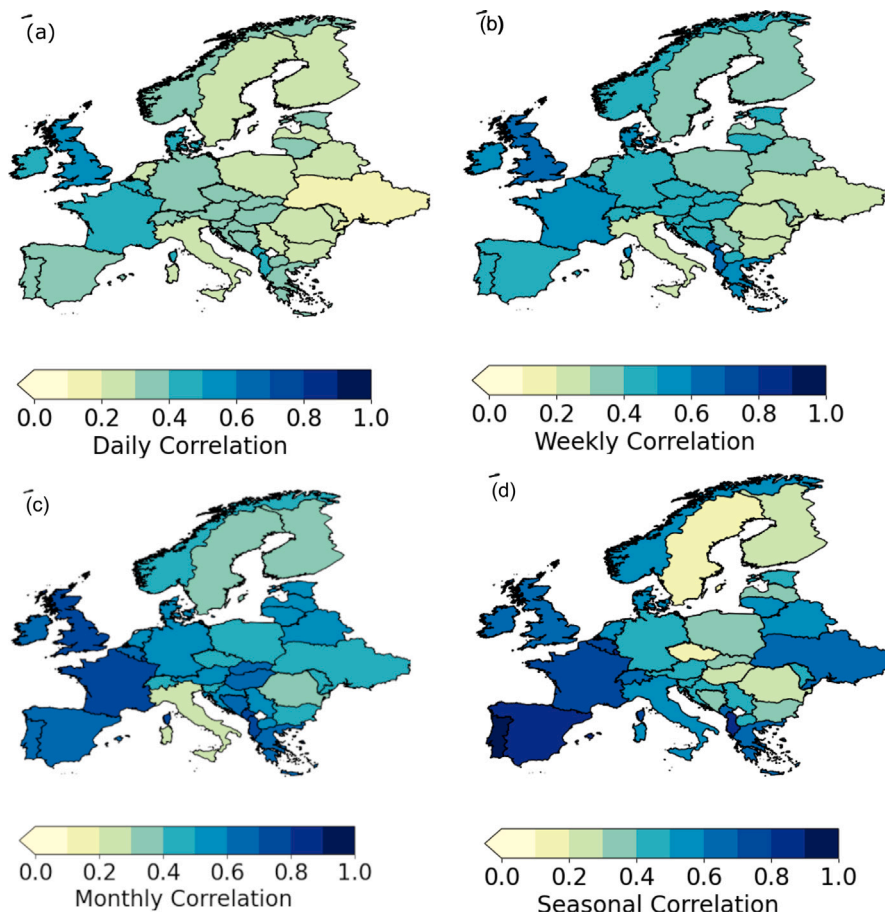|	Expected No.	Independently RP	No.	Historic ratio	RP	No.	Future ratio	RP
95%	102.6	2.2	246	2.4	0.7	553	5.3	0.4
99%	4.1	55.6	14	3.4	12.9	55	13.4	3.7

Fig. 6. Spearman's rank correlation between national-aggregate total river flows (GLOFAS) and mean maximum daily 10 m wind gusts (ERA5) over (a) daily (b) weekly, 7 days (c) monthly, 30 days (d) seasonal, 180 days timescales. Data are not population weighted.

climatology and the impact of flood defences (Tian et al., 2019). Flood protection, in particular, is ubiquitous along European rivers and is typically designed to prevent damage by events with a return period of up to 1 in 100 years, and possibly higher in particular locations (Buijs et al., 2007). However, such low frequency events are rare by definition and an FSI metric constructed only from historical daily river flows with 1% annual probability (i.e., 99.99998th percentile at a daily time scale) would have a few, if any non-zero data points. The short observational record (in our case ~40 years of ERA5 data) also creates a challenge for estimating very extreme behaviours, and the uncertainty on estimating these high percentile thresholds is very large.

Instead, for an effective FSI measure we select events that, whilst rare in the observational record, are sufficiently frequent to give a meaningful sample size and have a correlation that seems to reflect that of more extreme events that actually result in flood damage. This choice is a compromise. We select the 99.5th percentile in each grid box. We assume that larger and more widespread exceedance of this threshold will give a stronger indication of potential flood damage.

As a consequence of these arguments, and testing against historic occurrences (Section 3.2 and Appendix D), we believe that the novel FSI metric is useful. It reflects events with potential to cause impact, is readily computable from climate model data, and can be the basis of statistics (e.g., Table 2) in a form that may be useable by stakeholders across a range of sectors.

4.2. Timescales, and a conceptual model of GB co-occurrence

Reported correlations of extremes relating to flooding and wind damage in GB vary with timescale. Proposals to understand these observations in terms of physical processes (Hillier et al., 2015; De Luca et al., 2020; Hillier and Dixon, 2020; Owen et al., 2021b) have yet to be reconciled by integrating them into a conceptual model incorporating the main hydro-meteorological processes over GB.

This paper applied a consistent approach to a spectrum of time-windows and variety of data types to better understand whether co-occurrence is maximised at timescales associated with: (i) individual
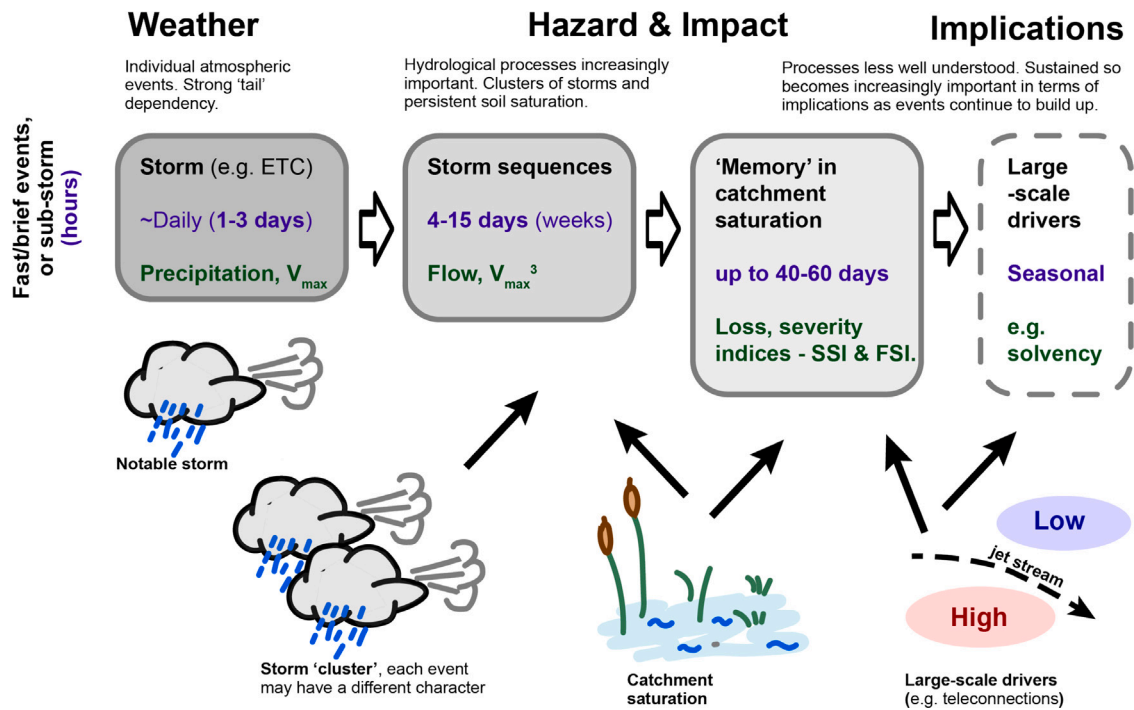
Fig. 7. Conceptual model of extremes related to UK wintertime flooding and wind damage. Key dimensions considered are time-scale (increasing left to right, purple text), proximity of the metric used to impact (green text), and the interplay of atmospheric and hydrological processes (graphics, black text). (For interpretation of the references to colour in this figure legend, the reader is referred to the web version of this article.)

storms (Fink et al., 2009; Liberato, 2014; Raveh-Rubin, 2015; Matthews et al., 2018; Otto et al., 2018; Owen et al., 2021b), (ii) the cluster-ing of storms within relatively short time windows (<14 days) that can saturate soils to create widespread flooding (Vitolo et al., 2009; Lavers et al., 2013; De Luca et al., 2017), or (iii) from persistence on climatological timescales to create wet and stormy winters (Matthews et al., 2014; Kendon and McCarthy, 2015; Palin et al., 2016; Hillier and Dixon, 2020).

A conceptual model of these driving processes is shown in Fig. 7. Timescale, progression from meteorological variables to impact, and physical processes are interwoven into an initial and necessarily sim-plified view that we hope will form the basis for debate.

Previous studies analysing individual storms (Fink et al., 2009; Liberato, 2014; Raveh-Rubin, 2015; Matthews et al., 2018; Otto et al., 2018) and systematic flood-wind correlation (Matthews et al., 2014; Hillier et al., 2015; Martius et al., 2016) were all based on an empir-ical presumption that extra-tropical cyclones (ETCs) are the dominant driver of wintertime hazard and risk. Such distinct, large scale weather phenomena, sets a key time-scale of ~1–3 days for co-occurrence. Across datasets, this analysis robustly confirms (Figs. 3 and 5) that there is strong co-occurrence ($r_s \sim 0.7$) for precipitation and wind gusts in this time frame. So, in line with abundant evidence that some storms can be both wet and windy, a large part, but not all, of this is attributed here to individual atmospheric events (Fig. 7, darkest grey box). The model also highlights that dependency appears to remain strong in the tail of the distribution at this timescale (Table 2, Fig. C.10a, d), something that is not required even if the bulk of events correlate.

There are a number of curiosities, however, to challenge this simple view. Hillier and Dixon (2020), demonstrate that storms impacting north-west GB either tend to be very wet or very windy, not extreme in both. They postulate that this is because storms with the most damaging winds are likely to still be actively interacting with the jet stream, but those with the most extreme rain are probably not. This explains the low daily correlation observed in ERA-interim (Martius et al., 2016), and their results showing 80%–90% of the impact of a link between

wind and rain extremes across a season comes from longer timescales than this in GB. In a mirror of this finding, at sub-storm timescales a peak in correlation is found at 1–2 h, descending to a 24–72 h window even as 70% of co-occurrences happen when an ETC is within 1000 km (Owen et al., 2021b). This pattern is confirmed and set in context by this paper's findings, with much lower on the correlations between precipitation and wind gusts at daily than weekly timescales (Fig. 3).

On weekly timescales (i.e., 4–15 days), historical data (Fig. 3) robustly demonstrate that co-occurrence for weather related variables (i.e. P, v^3) increases to peak at ~10 days. This increase on a timescale greater than a storm's residency over GB implies it is typically not just individual storms causing the correlation, strengthening support for this specific idea (Hillier et al., 2015; De Luca et al., 2017). More generally, these observations strongly support the postulate that persistence or 'memory' in the hydro-meteorological system is a critical part of the story (Hillier et al., 2015). The origin of the memory must be atmo-spheric, hydrological, or both, simply because these are the two sets of processes at work in GB. Three main possibilities have been suggested:

- Persistence in synoptic conditions such as jet stream position, the presence of atmospheric rivers (Lavers et al., 2011; Dacre and Pinto, 2020) or recurrent rossby wave packets (Ali et al., 2021) lasting from 3 days up to a few weeks, driving a multi-storm hazard (Priestley et al., 2018).
- Persistent large-scale flow patterns, such as the North Atlantic Oscillation (Feser et al., 2015; Hillier et al., 2015; Dacre and Pinto, 2020)
- Soil saturation in catchments (Kendon and McCarthy, 2015; Hillier et al., 2015; De Luca et al., 2017; Berghuijs et al., 2019)

It is well-established that ETCs can cluster, with several arriving across 1–2 weeks (Mailier et al., 2006; Vitolo et al., 2009), with a recent example over GB experienced in February 2022 (i.e., Dudley — wind North GB, Eunice — wind in South GB, Franklin — flooding in north GB). A key observation is that peak flows tend to occur 0–13 days

after very severe gales, interpreted as indicating that flooding occurs in the last of a few storms due to soil becoming saturated (De Luca et al., 2017). Use of hydrological modelling in this paper that includes soil wetness, water absorption, run-off and river flow (i.e., GLOFAS, G2G) greatly strengthens this hypothesis as it shows correlation rising from 0.4 (t = 1 day) to 0.6 by monthly timescales (∼0–60 days). Thus, catchment saturation is a key part of the model, although, we note that there will be variability between catchments.

On longer timescales, up to seasonal (180 days), compound risk appears to be elevated by persistent underlying environmental conditions (Hillier et al., 2015; De Luca et al., 2017; Hillier and Dixon, 2020), but understanding of processes gets significantly more speculative. In terms of atmospheric climate modes, positive North Atlantic Oscillation (NAO) has been proposed as it is a well-established as a condition favouring storminess in GB (Hillier and Dixon, 2020) although whether the cause is the long term average itself or a tendency to support more frequent and persistent episodes of high NAO conditions (i.e., >1.0) is not clear at present. It has also been postulated that persistence might be induced by teleconnections to the western Pacific warm pool (Huntingford et al., 2014; Hillier et al., 2015). Empirically, some role for long-term soil wetness is suggested since frequent very severe gales and the largest multi-basin floods coincide with enduringly wet conditions as recorded in standardised precipitation indices (De Luca et al., 2017).

A challenge remains to work out the details. Outstanding questions exist about all the time-scales upon which processes driving co-occurrence act, including:

- What causes individual storms lasting 1–2 days to produce flooding and extreme wind, as opposed to both or neither?
- What large-scale drivers lead to storm clusters capable of driving co-occurrence over sub-seasonal timescales?
- How exactly do catchment properties induce memory up to monthly timescales?
- Are the processes that govern the correlation at (3–6 month) timescales the same as those present at sub-seasonal timescales?

4.3. Future correlation

In agreement with past studies focused on historical precipitation and wind gusts (Martius et al., 2016; Owen et al., 2021b), there is broad similarity between correlation patterns for UKCP for 1981–2000 and historic observations (compare Figs. 3 and 5). Broadly, correlation in the future UKCP (2061–2080) at first appears similar, yet there is a development of enhanced co-occurrence for the more extreme short-timescale joint events (Table 2, Fig. 5b).

If true, an increase in jointly occurring very severe extremes of roughly threefold by 2061–2080 (p < 0.05), with commensurate decrease in return period from 13 to 4 years is dramatic. We note that UKCP regional simulations are based on one possible global climate model projection, for which multiple ensemble members are run under one high emissions scenario. Other global climate model projections also need to be investigated to determine how robust these initial results are.

As to the origin of the increased co-occurrence, we postulate that flooding driven by extreme precipitation is the limiting factor for a compound event. This originates in the temporal observation that large multi-basin floods (De Luca et al., 2017) tend to occur 0–13 days after a storm. This is consistent with the role of catchment saturation identified in this study and in Ledingham et al. (2019) for annual maximum rainfall vs. flood runoff. It is commonly a pre-condition for flooding, which extreme winds do not have, making flooding the limiting factor for co-occurrence. A similar argument applies spatially, based on this study's observation that the largest FSI events (top 0.1%) are more localised than SSI ones (Fig. 4), and are thus limiting. In addition the UKCP results show that with respect to the historical period (1980–2000) there is moderate decrease in SSI days in 2061–2080 (−2%) and

a similarly sized increase in days with an FSI (+ 3%), and it is easier to imagine the quantity that is increasing driving an increased level of co-occurrence. A similar result is seen by Yaddanapudi et al. (2022) in coastal regions when analysing wind and flood responses to climate change in CMIP6 simulations. More widely, support for this postulate comes from studies demonstrating a warmer and therefore wetter atmosphere (Lowe et al., 2018) and a likely increase in extreme precipitation associated with this (Chan et al., 2014; Kendon et al., 2020; Fowler et al., 2021) and increased high river flows (Kay et al., 2021; Griffin et al., 2022b). Future work could address the role of changing soil moisture in the occurrence of these compound events (incorporating results from Kay et al., 2022; Griffin et al., 2022b). Opportunities to link these results with present and futures changes in the spatial structure of the flood damage (e.g., taking account of existing flood defences and the local exposure of people and property) to provide more direct risk-based severity insights across multiple hazards also exist. All these aspects continue to evolve and are likely to be of most direct relevance to stakeholders.

4.4. Extending across Europe

Previous studies have shown maps of flood-wind relationships across Europe at daily (Martius et al., 2016; Owen et al., 2021b) or seasonal (Hillier and Dixon, 2020) timescale. Fig. 6 presents a more complete picture. The patterns in Fig. 6 allow an initial interpretation to be offered. On daily timescales, highest wind-river flow correlations are seen over GB and Ireland, likely due to their relatively isolated and therefore rapidly responding river networks.

At weekly and monthly timescales the countries in central and northern Europe which are commonly impacted by extra-tropical cyclones see highest correlations, with lower correlations over southern and eastern Europe. Indeed, high monthly correlations are seen in countries which experience significant storm clustering (Roberts et al., 2014; Priestley et al., 2018). The fact that Western Europe experiences stronger correlations on all timescales supports the analysis of Berghuijs et al. (2019) which shows the dominant driver of flooding over Western Europe being soil moisture processes, rather than extreme precipitation or snowmelt.

On seasonal timescales, highest correlation is seen over Spain and Portugal, which suggests the drivers causing extreme river flows are very similar to those causing extreme winds (see also Hénin et al., 2021). Generally low correlations are seen over Sweden and Finland at all timescales. Part of this is likely due to these countries being in the lee of mountains sheltered from passing cyclones in a *correlation shadow* (Hillier and Dixon, 2020). However, temperature and snow melt are known to strongly influence river flows here (Arheimer and Lindström, 2015; Berghuijs et al., 2019) which will reduce correlation as they are not directly related to storms and their extreme winds, and simple climate phenomena like the NAO may not be appropriate for describing processes in these regions (Kingston et al., 2009). Correlations are also lower than GB values for countries which have much larger river catchment areas (e.g., Germany). The explanation might be physical, or to do with our methods focus on country-level data. An approach based on event footprints may be needed in future work to capture behaviour in neighbouring countries.

It is important to note that different stakeholders are sensitive to correlations in different ways on a variety of time-frames (e.g., an event emergency response in <24 h, or event duration of up to 5 days defined in a reinsurance contract, or planning decisions relating to annual budgets or limits in a regulator's guidance).

5. Conclusions

Rank correlation has been consistently calculated for a spectrum of time-windows and variety of data types, to better understand how a variety of hydro-meteorological processes contribute to the co-occurrence

of extremes relating to flooding and wind damage. GB is used as a case study, which is subsequently extended to the European domain. From this the following main conclusions can be drawn:

- A new flood severity index (FSI), to complement the SSI metric for potential wind damage, is demonstrated to usefully represent potential flooding.
- GB's hydro-meteorological correlation ranges from 0.6–0.8 for most timescales, with notable differences between wind gusts vs. precipitation and wind gusts vs. river flow.
- Correlation drops significantly to 0.2–0.4 for impact-based measures focused on extremes (i.e., FSI, SSI).
- In a future climate, co-occurrence of most extreme events (i.e., FSI and SSI both exceeding the 99th percentile) becomes roughly threefold more frequent.
- Present day return periods of daily compound-wind flood events are reduced from 16.3 to 4.7 years, which is very much less than the 55.6 years expected if the two hazards occurred independently.
- Across Europe the timescales at which correlations peak varies depending on the local drivers of flood and wind damage.

This study presents the first large-scale application of hydrological modelling to the question of flood and wind co-occurrence using both the GLOFAS dataset and the UKCEH Grid-to-Grid models. Considering multiple timescales, and various pathways to the impact variables has allowed for insights into the processes driving co-occurrence across Europe. If a single take-home message is desired, it is that it is critical to represent the relationship between flooding and extreme wind within any risk modelling framework for insurers or infrastructure providers. This is already becoming a component of the UK General Insurers Stress Tests (BOE, 2022). The results also inform ongoing discussion about the appropriateness of climate data when these stress tests are designed (Albano et al., 2021; Qiu et al., 2022).

CRediT authorship contribution statement

Bloomfield H.C.: Conceptualization, Data curation, Formal analysis, Investigation, Methodology, Visualization, Writing – original draft, Writing – review & editing. **Hillier J.:** Conceptualization, Data curation, Formal analysis, Investigation, Methodology, Supervision, Writing – original draft, Writing – review & editing. **Griffin A.:** Data curation, Formal analysis, Writing – review & editing. **Kay A.L.:** Data curation, Formal analysis, Writing – review & editing. **Shaffrey L.C.:** Conceptualization, Funding acquisition, Methodology, Project administration, Writing – review & editing. **Pianosi F.:** Conceptualization, Funding acquisition, Writing – review & editing. **James R.:** Conceptualization, Funding acquisition, Writing – review & editing. **Kumar D.:** Writing – review & editing. **Champion A.:** Conceptualization, Writing – review & editing. **Bates P.D.:** Conceptualization, Funding acquisition, Methodology, Project administration, Writing – review & editing.

Declaration of competing interest

The authors declare the following financial interests/personal relationships which may be considered as potential competing interests:Hannah Bloomfield reports financial support was provided by Centre for Greening finance and investment. Hannah Bloomfield reports a relationship with Centre for Greening Finance and Investment that includes: employment and funding grants. John Hillier reports financial support was provided by ROBUST, NERC Knowledge Exchange Fellowship. John Hillier reports a relationship with ROBUST, NERC Knowledge Exchange Fellowship that includes: employment and funding grants.

Data availability

A list of the meteorological datasets used in this study is given in Table Table 1. ERA5 and GLOFAS can be downloaded from the Copernicus climate data store https://cds.climate.copernicus.eu/#!/home. The CAMELS-GB dataset is available from https://doi.org/10.5285/8344e4f3-d2ea-44f5-8afa-86d2987543a9. Information about downloading the CHESS-MET dataset can be found from the UK CEH Environmental Information Platform https://eip.ceh.ac.uk/. UKCP data was available through the JASMIN supercomputer. The UKCP-based GB river flow projections were developed in the AquaCAT project funded by UK Climate Resilience Programme and lead by Sayers and Partners in association with UKCEH.

A digital demonstrator showing wind-flood correlations from this study is available at https://the-iea.github.io/cgfi-wind-flood/.

Acknowledgements

Appendix A. Correlations in a different observational dataset

CAMELS-GB collates river flows, catchment attributes and catchment boundaries from the UK National River Flow Archive together with a suite of meteorological time series and catchment attributes, covering a period from 1970–2015. The catchment daily averaged total precipitation data are derived from CEH-GEAR (Keller et al., 2015) and catchment daily averaged wind speeds are from the CHESS-MET dataset (Robinson et al., 2016). Further details on CEH-GEAR and CHESS-MET can be found in the relevant papers, but the key point is these datasets provide gridded observations over the UK at 1 km resolution, derived from observation-based datasets from the UK Met Office and relevant river authorities in the UK's devolved nations.

Similar correlations were found for CAMELS-GB to those seen in Fig. 3a when using the 1980–2015 historical period (Fig. A.8a). We note the correlation between wind speeds and daily total precipitation is lower than seen for ERA5 by ~0.1, and the relationship between river flow and wind gusts is a bit stronger. The most noticeable different is seen for the FSI and SSI correlations, where a strong decay is seen in observations when aggregated to seasonal timescales.

The results are also similar when sub-setting to only use the 134 largest river catchments (i.e., the top 20%; Fig. A.8b). After subsetting the relationship between FSI and SSI looks more similar to that seen in ERA5 and GLOFAS in Fig. 3. Differences could be due to the locations of river flow measurements available through CAMELS (rather than the uniform approach taken when using ERA5 and GLOFAS) or due to the more localised representation of physical processes available from the observed datasets.

Further backward extensions were not possible due to trends found in the early (i.e.,1970–1980) wind speeds and precipitation data. These are believed to be due to limited earlier reporting as opposed to having a physical based, but are beyond the scope of this paper and not shown.
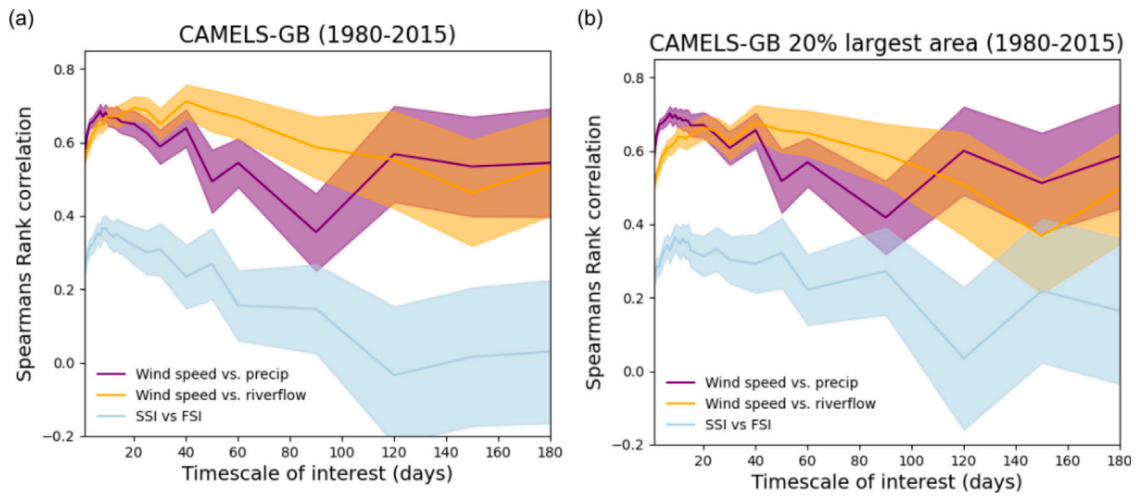
Fig. A.8. Spearman's rank correlation between various metrics, at various timescales from 1 to 180 days and aggregated across GB with precipitation and wind speeds taken from CHESS-MET and river flows taken from CAMELS-GB. Equal weighting is given to all grid boxes (as in Fig. 3). Shaded areas show two standard deviations of 2000 bootstrapped samples (95% confidence) of the correlations. Details of datasets used are given in Table 1.
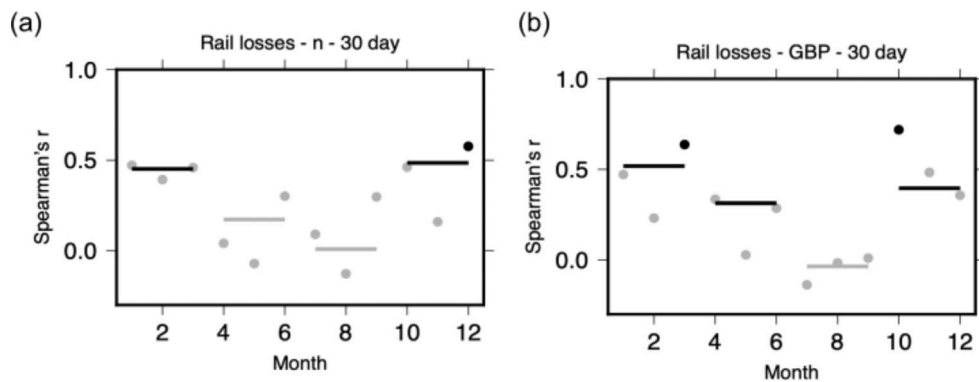

Fig. B.9. Spearman's rank correlation between Rail losses due to wind and flood for (a) Number of events (b) Costs incurred. Computation on monthly (dots) and seasonal (~90-day, dashes) timescales, with black indicating $p < 0.05$ despite only data from 2006–2018.

Appendix B. WRIID data quality

In other loss datasets, mis-categorisation of some losses is a recognised issue. For instance, in the Association of British Insurers (ABI) *General Insurance Statistics*, some pluvial inundation (surface water flooding) is known by practitioners to be sometimes reported as wind damage because it is associated with stormy weather; see Hillier et al. (2015) for further details. This reporting artefact makes it difficult tov reliably establish a correlation between flooding and extreme wind. Such an artefact does not appear to be present in the WRIID dataset (see Fig. B.9). In winter significant correlation is seen between flood and wind damage ($r_s \sim 0.5$, $p < 0.05$), but in summer there is no demonstrable relationship (Fig. B.9). It is difficult to imagine a reporting artefact which might exist in winter and yet be avoided in summer. So, this gives confidence that the winter-time relationships shown in Fig. 3c are real and not explored further here.

Appendix C. Suitability of Spearman's Rank correlation

By using ranks, Spearman's Rank (r_s) minimises the influence of the heavy-tailed marginal distributions typical of extremes, and also reduces sensitivity to the exact form of the metrics selected (e.g., whether wind speeds are cubed or not). Namely, it allows for comparison of results in the presence of non-linear relationships such as between meteorological variables and damage metrics. Whilst, r_s is simple, familiar and thus amenable for easy communication to varied stakeholders,

two variables X_1 and X_2 might be dependent and yet uncorrelated in the extremes (i.e., asymptotically independent, e.g., Heffernan and Tawn, 2004). Introduced by Coles et al. (1999), extremal correlation (χ) and residual tail dependence ($\bar{\chi}$) are used to understand asymptotic behaviour; see Vignotto et al. (2021) for a fuller mathematical description. χ presents the probability of one variable being extreme given that the other one is extreme, whereas $\bar{\chi}$ presents the strength of the relationship in the tails of the distribution. The point of presenting both of these statistics is that two variables can be dependent at the same time as being asymptotically independent ($\bar{\chi} < 1$). It is common to present χ and $\bar{\chi}$ as estimates for different percentile thresholds, and then visually inspect their behaviour as the thresholds become more extreme.

For meteorological variables, precipitation and wind gusts in ERA5, $\bar{\chi}$ is not converging towards 1, so the variables are asymptotically independent, yet neither is $\bar{\chi}$ obvious or rapidly nearing zero, so dependency remains present a notable depth into the distributions tail. This result holds for timescales from daily to monthly (Fig. C.10a–c). Similar is true for the relationship between distributions of ERA5 wind gusts and GLOFAS river flows (Fig. C.10d–f). This pattern continues across the spectrum from weather to impact, including for monthly Network Rail losses (not shown).

As there is no indication that correlation disappears moving from the body into the tail of the data, r_s is retained as the main statistic deployed. These statistics have been computed using R's *taildep()* function from the extRemes package (Gilleland and Katz, 2016). Aggregated at
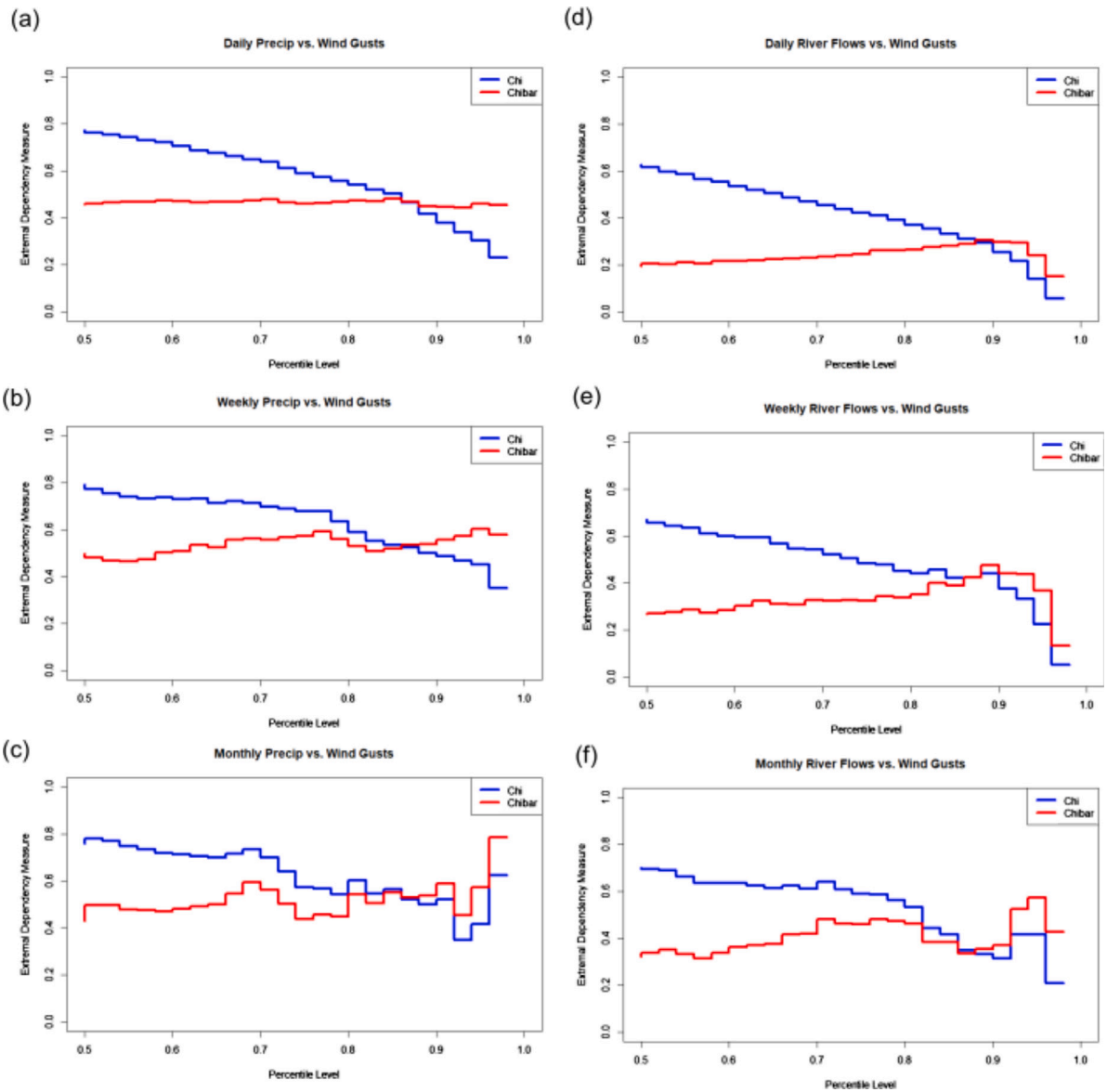
Fig. C.10. Residual tail dependency analysis for ERA5 precipitation vs. ERA5 wind gusts (left) and GLOFAS river flows vs. ERA5 wind gusts (right) for daily (top) weekly (middle) and monthly (bottom) timescales.
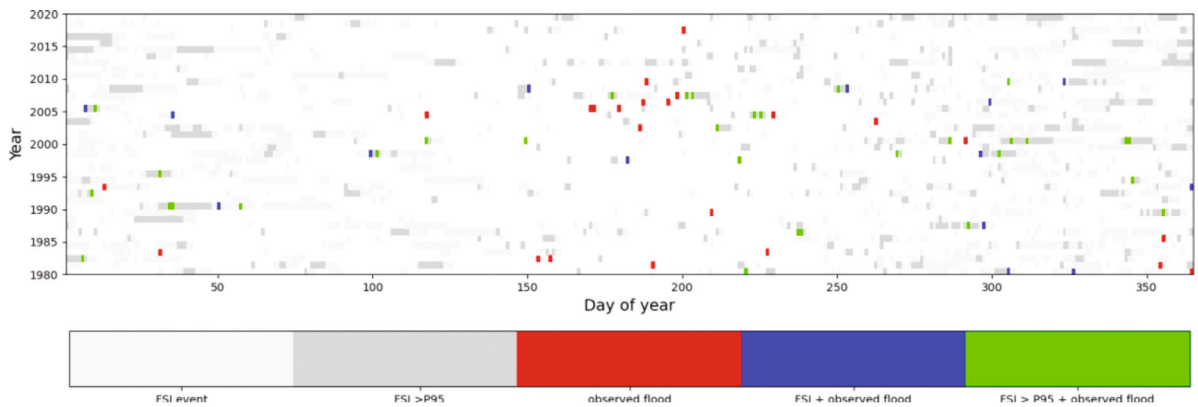

Fig. D.11. Verification of GLOFAS FSI metric when compared to the flood chronology from Black and Law (2004). (For interpretation of the references to colour in this figure legend, the reader is referred to the web version of this article.)

GB level, <0.5% of days in the ERA5 data have zero precipitation, so zeros and tied ranks do not alter the results.

Appendix D. Performance of the FSI metric

To provide confidence that the FSI metric is able to reproduce notable events from the historical record, the time series of FSI generated from GLOFAS is compared to a national web-based chronology of hydrological events (Black and Law, 2004). The comparisons have been made here for GLOFAS but very similar results are seen for FSI's computed for CAMELS-GB (not shown).

Fig. D.11 shows where FSI events were captured within the time period for which the flood chronology is available (1980–2020). The FSI metric picks up numerous small events where no flooding was recorded across GB (grey points in Fig. D.11). However, the FSI metric captures a large percentage of the winter floods recorded (28 out of 34 events) with the FSI of these often exceeding the 95th percentile (green points). Events defined by FSI tend to last for a few days either side of the reported flooding.

The FSI struggles to capture the summer flooding events. These often happen in very small, flashier catchments and may be difficult for GLOFAS to represent. However, 19 out of 37 summer floods are captured by GLOFAS, which is a respectable proportion. As summer flooding was not the focus of the study, the reasons they are not effectively captured have not been investigated further.

References

ABI, Association of Bristish Insurers, 2014. Data: 'General Insurance Statistics'. URL https://www.abi.org.uk/data/free-industry-data-downloads/.

Albano, C.M., McCarthy, M.I., Dettinger, M.D., McAfee, S.A., 2021. Techniques for constructing climate scenarios for stress test applications. Clim. Change 164 (3), 1–25. http://dx.doi.org/10.1007/s10584-021-02985-6.

Ali, S.M., Martius, O., Röthlisberger, M., 2021. Recurrent rossby wave packets modulate the persistence of dry and wet spells across the globe. Geophys. Res. Lett. 48 (5), http://dx.doi.org/10.1029/2020GL091452, e2020GL091452.

Arheimer, B., Lindström, G., 2015. Climate impact on floods: changes in high flows in Sweden in the past and the future (1911–2100). Hydrol. Earth Syst. Sci. 19 (2), 771–784. http://dx.doi.org/10.5194/hess-19-771-2015.

Berghuijs, W.R., Harrigan, S., Molnar, P., Slater, L., Kirchner, J.W., 2019. The relative importance of different flood-generating mechanisms across Europe. Water Resour. Res. 55 (6), 4582–4593. http://dx.doi.org/10.1029/2019WR024841.

Bevacqua, E., De Michele, C., Manning, C., Couasnon, A., Ribeiro, A.F.S., Ramos, A.M., Vignotto, E., Bastos, A., Blesic, S., Durante, F., Hillier, J.K., Oliveira, S.C., Pinto, J.G., Ragno, E., Rivoire, P., Saunders, K., van der Wiel, K., Wu, W., Zhang, T., Zscheischler, J., 2021. Guidelines for studying diverse types of compound weather and climate events. Earth's Future 9 (11), http://dx.doi.org/10.1029/2021EF002340, e2021EF002340.

Black, A.R., Law, F.M., 2004. Development and utilization of a national web-based chronology of hydrological events/Développement et utilisation sur internet d'une chronologie nationale d'événements hydrologiques. Hydrol. Sci. J. 49 (2), http://dx.doi.org/10.1623/hysj.49.2.237.34835.

BOE, B.o.E.., 2022. Insurance stress test 2022 – request for technical input. URL https://www.bankofengland.co.uk/prudential-regulation/letter/2022/january/insurance-stress-test-2022-request-for-technical-input.

Buijs, F., Simm, J., Wallis, M., Sayers, P., 2007. Performance and Reliability of Flood and Coastal Defences. Environment Agency, London.

Chan, S., Kendon, E., Fowler, H., Blenkinsop, S., Roberts, N., 2014. Projected increases in summer and winter UK sub-daily precipitation extremes from high-resolution regional climate models. Environ. Res. Lett. 9 (8), 084019. http://dx.doi.org/10.1088/1748-9326/9/8/084019.

Coles, S., Heffernan, J., Tawn, J., 1999. Dependence measures for extreme value analyses. Extremes 2 (4), 339–365. http://dx.doi.org/10.1023/A:1009963131610.

Cotterill, D., Stott, P., Christidis, N., Kendon, E., 2021. Increase in the frequency of extreme daily precipitation in the United Kingdom in autumn. Weather Clim. Extremes 33, 100340. http://dx.doi.org/10.1016/j.wace.2021.100340.

Coxon, G., Addor, N., Bloomfield, J.P., Freer, J., Fry, M., Hannaford, J., Howden, N.J., Lane, R., Lewis, M., Robinson, E.L., et al., 2020. CAMELS-GB: Hydrometeorological time series and landscape attributes for 671 catchments in great britain. Earth Syst. Sci. Data 12 (4), 2459–2483. http://dx.doi.org/10.5194/essd-12-2459-2020.

Dacre, H.F., Pinto, J.G., 2020. Serial clustering of extratropical cyclones: A review of where, when and why it occurs. NPJ Climate Atmospheric Sci. 3 (1), 1–10. http://dx.doi.org/10.1038/s41612-020-00152-9.

De Luca, P., Hillier, J.K., Wilby, R.L., Quinn, N., Harrigan, S., 2017. Extreme multi-basin flooding linked with extra-tropical cyclones. Env. Res. Lett. 12 (11), 114009. http://dx.doi.org/10.1088/1748-9326/aa868e.

De Luca, P., Messori, G., Pons, F.M.E., Faranda, D., 2020. Dynamical systems theory sheds new light on compound climate extremes in Europe and Eastern North America. Quart. J. Royal Meteorol. Soc. http://dx.doi.org/10.1002/qj.3757.

Doxsey-Whitfield, E., MacManus, K., Adamo, S.B., Pistolesi, L., Squires, J., Borkovska, O., Baptista, S.R., 2015. Taking advantage of the improved availability of census data: a first look at the gridded population of the world, version 4. Papers Appl. Geogr. 1 (3), 226–234. http://dx.doi.org/10.1080/23754931.2015.1014272.

Ferranti, E.J.S., Chapman, L., Lowe, C., McCulloch, S., Jaroszweski, D., Quinn, A.D., 2016. Heat-related failures on South-East England's railway network: insights and implications for heat-risk management. Weather Clim. Soc. 8, 177–191. http://dx.doi.org/10.1175/WCAS-D-15-0068.1.

Ferranti, E.J.S., Jaroszweski, D., Lee, S., Chapman, L., Lowe, C., Quinn, A.D., 2018. The hottest july day on the railway network: insights and thoughts for the future. Meteorol. Appl. 5, 195–208. http://dx.doi.org/10.1002/met.1681.

Feser, F., Barcikowska, M., Krueger, O., Schenk, F., Weisse, R., Xia, L., 2015. Storminess over the North Atlantic and northwestern Europe—A review. Q. J. R. Meteorol. Soc. 141 (687), 350–382. http://dx.doi.org/10.1002/qj.2364.

Fink, A.H., Brucher, T., Ermert, V., Kruger, A., Pinto, J.G., 2009. The European storm Kyrill in January 2007: Synoptic evolution, meteorological impacts and some considerations with respect to climate change. Nat. Hazards Earth Syst. Sci. 9, 405–423. http://dx.doi.org/10.5194/nhess-9-405-2009.

Fowler, H.J., Lenderink, G., Prein, A.F., Westra, S., Allan, R.P., Ban, N., Barbero, R., Berg, P., Blenkinsop, S., Do, H.X., et al., 2021. Anthropogenic intensification of short-duration rainfall extremes. Nat. Rev. Earth Environ. 2 (2), 107–122. http://dx.doi.org/10.1038/s43017-020-00128-6.

Gilleland, E., Katz, R.W., 2016. extRemes 2.0: An extreme value analysis package in R. J. Stat. Softw. 72 (8), 1–39. http://dx.doi.org/10.18637/jss.v072.i08.

Griffin, A., Kay, A., Bell, V., Stewart, E., Sayers, P., Carr, S., 2022a. Peak flow and probability of exceedance data for grid-to-grid modelled widespread flooding events across mainland GB from 1980–2010 and 2050–2080. http://dx.doi.org/10.5285/26ce15dd-f994-40e0-8a09-5f257cc1f2ab.

Griffin, A., Kay, A., Sayers, P., Bell, V., Stewart, E., Carr, S., 2022b. Widespread flooding dynamics changing under climate change: characterising floods using UKCP18. Hydrol. Earth Syst. Sci. Discuss. 1–18. http://dx.doi.org/10.5194/hess-2022-243.

Harrigan, S., Zoster, E., Cloke, H., Salamon, P., Prudhomme, C., 2020. Daily ensemble river discharge reforecasts and real-time forecasts from the operational global flood awareness system. Hydrol. Earth Syst. Sci. Discuss. 1–22. http://dx.doi.org/10.5194/hess-27-1-2023.

Heffernan, J., Tawn, J., 2004. A conditional approach for multivariate extreme values. J. R. Stat. Soc. B 66 (3), 169–182. http://dx.doi.org/10.1111/j.1467-9868.2004.02050.x.

Hénin, R., Ramos, A.M., Pinto, J.G., Liberato, M.L., 2021. A ranking of concurrent precipitation and wind events for the Iberian Peninsula. Int. J. Climatol. 41 (2), 1421–1437. http://dx.doi.org/10.1002/joc.6829.

Hersbach, H., Bell, B., Berrisford, P., Hirahara, S., Horányi, A., Muñoz-Sabater, J., Nicolas, J., Peubey, C., Radu, R., Schepers, D., et al., 2020. The ERA5 global reanalysis. Q. J. R. Meteorol. Soc. 146 (730), 1999–2049. http://dx.doi.org/10.1002/qj.3803.

Hillier, J.K., Dixon, R., 2020. Seasonal impact-based mapping of compound hazards. Env. Res. Lett. 15, 114013. http://dx.doi.org/10.1088/1748-9326/abbc3d.

Hillier, J.K., Macdonald, N., Leckebusch, G.C., Stavrinides, A., 2015. Interactions between apparently primary weather-driven hazards and their cost. Env. Res. Lett. 10, 104003. http://dx.doi.org/10.1088/1748-9326/10/10/104003.

Hillier, J.K., Matthews, T., Wilby, R.L., Murphy, C., 2020. Multi-hazard dependencies can increase and decrease risk. Nature Clim. Change 10, 595–598. http://dx.doi.org/10.1038/s41558-020-0832-y.

Hirpa, F.A., Salamon, P., Beck, H.E., Lorini, V., Alfieri, L., Zsoter, E., Dadson, S.J., 2018. Calibration of the Global Flood Awareness System (GloFAS) using daily streamflow data. J. Hydrol. 566, 595–606. http://dx.doi.org/10.1016/j.jhydrol.2018.09.052.

Huntingford, C., Marsh, T., Scaife, A.A., Kendon, E.J., 2014. Potential influences on the United Kingdom's floods of winter 2013/14. Nature Clim. Change 4, 769–777. http://dx.doi.org/10.1038/nclimate2314.

Jacob, D., Petersen, J., Eggert, B., Alias, A., Christensen, O.B.s., Bouwer, L.M., Braun, A., Colette, A., Déqué, M., Georgievski, G., et al., 2014. EURO-CORDEX: new high-resolution climate change projections for European impact research. Reg. Environ. Change 14 (2), 563–578. http://dx.doi.org/10.1007/s10113-013-0499-2.

Kay, A., 2021. Simulation of river flow in Britain under climate change: baseline performance and future seasonal changes. Hydrol. Process. 35, e14137. http://dx.doi.org/10.1002/hyp.14137.

Kay, A., Griffin, A., Rudd, A., Chapman, R., Bell, V., Arnell, N., 2021. Climate change effects on indicators of high and low river flow across Great Britain. Adv. Water Resour. 151, 103909. http://dx.doi.org/10.1016/j.advwatres.2021.103909.

Kay, A., Lane, R., Bell, V., 2022. Grid-based simulation of soil moisture in the UK: future changes in extremes and wetting and drying dates. Environ. Res. Lett. 17 (7), 074029. http://dx.doi.org/10.1088/1748-9326/ac7a4e.

Keller, V., Tanguy, M., Prosdocimi, I., Terry, J., Hitt, O., Cole, S., Fry, M., Morris, D., Dixon, H., 2015. CEH-GEAR: 1 km resolution daily and monthly areal rainfall estimates for the UK for hydrological and other applications. Earth Syst. Sci. Data 7 (1), 143–155. http://dx.doi.org/10.5194/essd-7-143-2015.

Kendon, M., McCarthy, M., 2015. The UK's wet and stormy winter of 2013/2014. Weather 7 (2), 40–47. http://dx.doi.org/10.1002/wea.2465.

Kendon, E.J., Roberts, N.M., Fosser, G., Martin, G.M., Lock, A.P., Murphy, J.M., Senior, C.A., Tucker, S.O., 2020. Greater future UK winter precipitation increase in new convection-permitting scenarios. J. Clim. 33 (17), 7303–7318. http://dx.doi.org/10.1175/JCLI-D-20-0089.1.

Kingston, D.G., Hannah, D.M., Lawler, D.M., McGregor, G.R., 2009. Climate–river flow relationships across montane and lowland environments in northern Europe. Hydrol. Process.: Int. J. 23 (7), 985–996. http://dx.doi.org/10.1002/hyp.7202.

Klawa, M., Ulbrich, U., 2003a. A model for the estimation of storm losses and the identification of severe winter storms in Germany. Nat. Hazards Earth Syst. Sci. 3 (6), 725–732. http://dx.doi.org/10.5194/nhess-3-725-2003.

Lane, R.A., Kay, A.L., 2021. Climate change impact on the magnitude and timing of hydrological extremes across Great Britain. Front. Water 71. http://dx.doi.org/10.3389/frwa.2021.684982.

Lavers, D.A., Allan, R.P., Villarini, G., Lloyd-Hughes, B., Brayshaw, D.J., Wade, A.J., 2013. Future changes in atmospheric rivers and their implications for winter flooding in Britain. Environ. Res. Lett. 8 (3), 034010. http://dx.doi.org/10.1088/1748-9326/8/3/034010.

Lavers, D.A., Allan, R.P., Wood, E.F., Villarini, G., Brayshaw, D.J., Wade, A.J., 2011. Winter floods in Britain are connected to atmospheric rivers. Geophys. Res. Lett. 38, L23803. http://dx.doi.org/10.1029/2011GL049783.

Ledingham, J., Archer, D., Lewis, E., Fowler, H., Kilsby, C., 2019. Contrasting seasonality of storm rainfall and flood runoff in the UK and some implications for rainfall-runoff methods of flood estimation. Hydrol. Res. 50 (5), 1309–1323. http://dx.doi.org/10.2166/nh.2019.040.

Li, D., Chen, Y., Messmer, M., Zhu, Y., Feng, J., Yin, B., Bevacqua, E., 2022. Compound wind and precipitation extremes across the indo-Pacific: Climatology, variability, and drivers. Geophys. Res. Lett. 49 (14), http://dx.doi.org/10.1029/2022GL098594, e2022GL098594.

Liberato, M.L.R., 2014. The 19 January 2013 windstorm over the North Atlantic: Large-scale dynamics and impacts on Iberia. Weather Clim. Extremes 5–6, 16–28. http://dx.doi.org/10.1016/j.wace.2014.06.002.

Lowe, J.A., Bernie, D., Bett, P., Bricheno, L., Brown, S., Calvert, D., Clark, R., Eagle, K., Edwards, T., Fosser, G., et al., 2018. UKCP18 Science Overview Report, Met Office Hadley Centre, Exeter, UK.

Mailier, P.J., Stephenson, D.B., Ferro, C.A., Hodges, K.I., 2006. Serial clustering of extratropical cyclones. Mon. Weather Rev. 134 (8), 2224–2240. http://dx.doi.org/10.1175/MWR3160.1.

Manning, C., Kendon, E.J., Fowler, H.J., Roberts, N.M., Berthou, S., Suri, D., Roberts, M.J., 2021. Extreme windstorms and sting jets in convection-permitting climate simulations over europe. Clim. Dynam. 1–18. http://dx.doi.org/10.1007/s00382-021-06011-4.

Martius, O., Pfahl, S., Chevalier, C., 2016. A global quantification of compound precipitation and wind extremes: Compound precipitation and wind extremes. Geophys. Res. Lett. 43, 7709–7714. http://dx.doi.org/10.1002/2016GL070017.

Matthews, T., Murphy, C., McCarthy, G., Broderik, C., Wilby, R.L., 2018. Super Storm Desmond: a process-based assessment. Env. Res. Lett. 13 (1), 014024. http://dx.doi.org/10.1088/1748-9326/aa98c8.

Matthews, T., Murphy, C., Wilby, R.L., Harrigan, S., 2014. Stormiest winter on record for Ireland and UK. Nature Clim. Change 4, 738–740. http://dx.doi.org/10.1038/nclimate2336.

Mitchell-Wallace, K., Jones, M., Hillier, J.K., Foote, M., 2017. Natural Catastrophe Risk Management and Modelling: A Practitioner's Guide. Wiley, Oxford, UK.

Otto, F., van der Wiel, K., van Oldenborgh, G.J., 2018. Climate change increases the probability of heavy rains in Northern England/Southern Scotland like those of storm Desmond-a real-time event attribution revisited. Environ. Res. Lett. 13 (2), 024006. http://dx.doi.org/10.1088/1748-9326/aa9663.

Owen, L.E., Catto, J.L., Dunstone, N.J., Stephenson, D.B., 2021a. How well can a seasonal forecast system represent three hourly compound wind and precipitation extremes over Europe? Environ. Res. Lett. 16 (7), 074019. http://dx.doi.org/10.1088/1748-9326/ac092e.

Owen, L.E., Catto, J.L., Stephenson, D.B., Dunstone, N.J., 2021b. Compound precipitation and wind extremes over europe and their relationship to extratropical cyclones. Weather Clim. Extremes 33, 100342. http://dx.doi.org/10.1016/j.wace.2021.100342.

Palin, E.J., Scaife, A.A., Wallace, E., Pope, E., Arribas, A., Brookshaw, A., 2016. Skillful seasonal forecasts of winter disruption to the U.K. transport system. J. Appl. Meteorol. Climatol. 55, 325–344. http://dx.doi.org/10.1175/JAMC-D-15-0102.1.

Pinto, J.G., Karremann, M.K., Born, K., Della-Marta, P.M., Klawa, M., 2012. Loss potentials associated with European windstorms under future climate conditions. Clim. Res. 54 (1), 1–20. http://dx.doi.org/10.3354/cr01111.

Priestley, M.D.K., Dacre, H.F., Shaffrey, L., Hodges, K.I., Pinto, J.G., 2018. The role of serial European windstorm clustering for extreme seasonal losses as determined from multi-centennial simulations of high-resolution global climate model data. Nat. Hazards Earth Syst. Sci. 18, 2991–3006. http://dx.doi.org/10.5194/nhess-18-2991-2018.

Qiu, J., Liu, B., Yang, F., Wang, X., He, X., 2022. Quantitative stress test of compound coastal-fluvial floods in China's pearl River Delta. Earth's Future http://dx.doi.org/10.1029/2021EF002638, e2021EF002638.

Quinn, N., Bates, P.D., Neal, J., Smith, A., Wing, O., Sampson, C., Smith, J., Heffernan, J., 2019. The spatial dependence of flood hazard and risk in the United States. Water Resour. Res. 55 (3), 1890–1911. http://dx.doi.org/10.1029/2018WR024205.

Raveh-Rubin, 2015. Large-scale wind and precipitation extremes in the Mediterranean: A climatological analysis for 1979–2012. Q. J. R. Meteorol. Soc. 141, 2404–2417. http://dx.doi.org/10.1002/qj.2531.

Ridder, N.N., Pitman, A.J., Ukkola, A.M., 2021. Do CMIP6 climate models simulate global or regional compound events skillfully? Geophys. Res. Lett. 48 (2), http://dx.doi.org/10.1029/2020GL091152, e2020GL091152.

Ridder, N.N., Pitman, A.J., Ukkola, A.M., 2022. High impact compound events in Australia. Weather Clim. Extremes 36, 100457. http://dx.doi.org/10.1016/j.wace.2022.100457.

Roberts, J.F., Champion, A.J., Dawkins, L.C., Hodges, K.I., Shafferty, L., Stephenson, D.S., Stringer, M.A., Thronton, H.E., Youngman, B.D., 2014. The XWS open access catalogue of extreme European windstorms from 1979–2012. Nat. Hazards Earth Syst. Sci. 14, 2487–2501. http://dx.doi.org/10.5194/nhess-14-2487-2014.

Robinson, E., Blyth, E., Clark, D., Comyn-Platt, E., Finch, J., Rudd, A., 2016. Climate hydrology and ecology research support system meteorology dataset for Great Britain (1961–2015)[CHESS-met]. http://dx.doi.org/10.5285/b745e7b1-626c-4ccc-ac27-56582e77b900.

Thompson, V., 2017. High risk of unprecedented UK rainfall in the current climate. Nature Commun. 8, 107. http://dx.doi.org/10.1038/s41467-017-00275-3.

Tian, X., Schleiss, M., Bouwens, C., van de Giesen, N., et al., 2019. Critical rainfall thresholds for urban pluvial flooding inferred from citizen observations. Sci. Total Environ. 689, 258–268. http://dx.doi.org/10.1016/j.scitotenv.2019.06.355.

Tucker, S.O., Kendon, E.J., Bellouin, N., Buonomo, E., Johnson, B., Murphy, J.M., 2022. Evaluation of a new 12 km regional perturbed parameter ensemble over europe. Clim. Dynam. 58 (3), 879–903. http://dx.doi.org/10.1007/s00382-021-05941-3.

Vignotto, E., Engelke, S., Zscheischler, J., 2021. Clustering bivariate dependencies of compound precipitation and wind extremes over Great Britain and Ireland. Weather Clim. Extremes 32, 100318.

Vitolo, R., Stephenson, D.S., Cook, I., Mitchell-Wallace, K., 2009. Serial clustering of intense European storms. Meteorol. Z. 18 (4), 411–424. http://dx.doi.org/10.1127/0941-2948/2009/0393.

White, C.J., Domeisen, D.I., Acharya, N., Adefisan, E.A., Anderson, M.L., Aura, S., Balogun, A.A., Bertram, D., Bluhm, S., Brayshaw, D.J., et al., 2022. Advances in the application and utility of subseasonal-to-seasonal predictions. Bull. Am. Meteorol. Soc. 103 (6), E1448–E1472. http://dx.doi.org/10.1175/BAMS-D-20-0224.1.

Williams, G.P., 1978. Bank-full discharge of rivers. Water Resour. Res. 14 (6), 1141–1154. http://dx.doi.org/10.1029/WR014i006p01141.

Yaddanapudi, R., Mishra, A., Huang, W., Chowdhary, H., 2022. Compound wind and precipitation extremes in global coastal regions under climate change. Geophys. Res. Lett. 49 (15), http://dx.doi.org/10.1029/2022GL098974, e2022GL098974.

Zscheischler, J., Naveau, P., Martius, O., Engelke, S., Raible, C.C., 2021. Evaluating the dependence structure of compound precipitation and wind speed extremes. Earth Syst. Dyn. 12 (1), 1–16. http://dx.doi.org/10.5194/esd-12-1-2021.